Investigation of the α_1-Glycine Receptor Channel-Opening Kinetics in the Submillisecond Time Domain

Christof Grewer

Max-Planck-Institut for Biophysics, D-60596 Frankfurt, Germany

ABSTRACT   The activation and desensitization kinetics of the human α_1-homooligomeric glycine receptor, which was transiently expressed in HEK 293 cells, were studied with a 100-μs time resolution to determine the rate and equilibrium constants of individual receptor reaction steps. Concentration jumps of the activating ligands glycine and β-alanine were initiated by photolysis of caged, inactive precursors and were followed by neurotransmitter binding, receptor-channel opening, and receptor desensitization steps that were separated along the time axis. Analysis of the ligand concentration-dependence of these processes allows the determination of 1) the rate constants of glycine binding, $k_{+1} \sim 10^7 \ M^{-1} \ s^{-1}$, and dissociation, $k_{-1} = 1900 \ s^{-1}$; 2) the rates of receptor-channel opening, $k_{op} = 2200 \ s^{-1}$, and closing, $k_{cl} = 38 \ s^{-1}$; 3) the receptor desensitization rate, $\alpha = 0.45 \ s^{-1}$; 4) the number of occupied ligand binding sites necessary for receptor-channel activation and desensitization, $n \geq 3$; and 5) the maximum receptor-channel open probability, $p_0 > 0.95$. The kinetics of receptor-channel activation are insensitive to the transmembrane potential. A general model for glycine receptor activation explaining the experimental data consists of a sequential mechanism based on rapid ligand-binding steps preceding a rate-limiting receptor-channel opening reaction and slow receptor desensitization.

INTRODUCTION

The strychnine-sensitive glycine receptor, which is expressed in high density in the spinal cord and the brainstem (Langosch et al., 1990), mediates fast inhibitory neurotransmission (Werman et al., 1968; for a recent review see Breitinger and Becker, 1998). Activation of the postsynaptic receptors by glycine leads to a transient chloride permeability increase of the postsynaptic membrane (Bormann et al., 1987; Coombs et al., 1955), which is accompanied by a change of the transmembrane potential toward the chloride equilibrium potential (Kandel et al., 1995). At the synapse these processes occur in the millisecond (ms) time region. The time course of the transmembrane potential change is determined by 1) the concentration of the neurotransmitter in the synaptic cleft as a function of time (Clements, 1996), and 2) the probability of open receptor-channels as a function of time and neurotransmitter concentration, $P_0(t, L)$ (Hess, 1993). The measurement of the equilibrium and rate constants, which determine $P_0(t, L)$, is, therefore, important. The rate constant of receptor-channel closing, k_{cl}, can be conveniently measured using the single-channel recording technique (Neher and Sakmann, 1976). In contrast, the exact determination of the receptor-channel opening rate, k_{op}, (Madsen and Edeson, 1988) and the intrinsic value of the dissociation constant of glycine from the receptor, K_1, (Colquhoun and Farrant, 1993) is difficult. A variety of methods was used to solve this problem; however, in case of the nicotinic acetylcholine receptor the results varied by two

orders of magnitude (reviewed by Hess, 1993; Madsen and Edeson, 1988). In order to accurately determine these parameters it is necessary to use rapid chemical reaction techniques with a submillisecond time resolution, making it possible to separate individual receptor reaction steps on the time axis (Matsubara et al., 1992).

A rapid chemical kinetic technique, the laser-pulse photolysis technique, was used recently to study activation (Matsubara et al., 1992; Hess, 1993) and inhibition (Grewer and Hess, 1999; Niu and Hess, 1993) of neurotransmitter receptors. The technique makes use of photolabile, inactive precursors of neurotransmitters. The precursor can be photolyzed on a submillisecond time scale with a pulse of laser light to generate the free neurotransmitter and the inactive protecting group (Billington et al., 1992). This method is used in conjunction with rapid solution exchange techniques to equilibrate receptors with caged or free neurotransmitter, respectively. By using this technique it was possible to determine the receptor-channel opening and closing rate constants of the muscle-type nicotinic acetylcholine receptor (Matsubara et al., 1992) as well as of the inhibitory γ-aminobutyric acid (GABA$_A$) receptor (Jayaraman and Hess, 1998). In case of the GABA$_A$ receptor, which was studied in rat hippocampal neurons, two populations of receptors with different opening and desensitizing kinetics were found. However, investigations of rapid reaction steps in the glycine receptor activation process using the laser-pulse photolysis technique were not possible because of the lack of suitable caged glycine derivatives. Recently, three new caged glycine receptor ligands were developed. They are based on two different caging groups, the 2-methoxy-5-nitrophenyl (MNP) group (Ramesh et al., 1993; Niu et al., 1996a) and the α-carboxy-2-nitrobenzyl (αCNB) group (Milburn et al., 1989; Grewer, Jäger, Carpenter, and Hess, unpublished results). These compounds photolyze with suf-

ficiently high rate constants ($>10^5$ s^{-1}) and quantum yield (>0.2) and they are biologically inert. They provide the necessary tools for the investigation of glycine receptor reactions on a submillisecond time scale.

Native glycine receptors expressed in rat primary neurons were extensively studied with rapid solution exchange methods combined with whole-cell current recording as well as single-channel recording (Bormann et al., 1987; Walstrom and Hess, 1994; Twyman and Macdonald, 1991). However, very little information about the kinetics of rapid receptor activation is available at present (Legendre, 1998; Harty and Manis, 1998). Estimates of the receptor-channel closing rate constant can be obtained from single-channel current-recording experiments (Takahashi et al., 1992) as well as decay times of glycinergic inhibitory postsynaptic currents (Stuart and Redman, 1990). In contrast, the rate constant of receptor-channel opening, k_{op}, is not known. No rapid chemical kinetic experiments have been performed with recombinant receptors in heterologous expression systems. Such systems have the advantage of defined receptor subtype and subunit composition. The α_1-subtype of the glycine receptor can serve as a model system because it 1) forms functional glycine-gated chloride channels (Langosch et al., 1990), and 2) is easily expressed in mammalian cells (Sontheimer et al., 1989). The goal of this work was to study the receptor-channel activation kinetics of the α_1-subtype of the inhibitory glycine receptor transiently expressed in HEK293 cells and to determine, for the first time, the rate constant of receptor-channel opening. For this purpose, the laser-pulse photolysis technique was used.

MATERIALS AND METHODS

Synthesis

α-Carboxy-o-nitrobenzyl-glycine ester (αCNB-glycine) was a kind gift from G. P. Hess (Cornell University, Ithaca, NY). 2-Methoxy-5-nitrophenyl glycine (MNP-glycine) and β-alanine (MNP-β-alanine) were synthesized according to published procedures (Ramesh et al., 1993; Niu et al., 1996a). Briefly, a solution of 1 mmol N-boc-glycine or β-alanine, 1 mmol dicyclohexylcarbodiimide, and 1 mmol 2-methoxy-5-nitrophenol in 7 ml methylene chloride was cooled in ice water and allowed to warm up to room temperature overnight under continuous stirring. The precipitate was removed and the remaining solution evaporated in vacuo. The residue was recrystallized from EtOH and dissolved in trifluoroacetic acid. After 10 min the deprotected 2-methoxy-5-nitrophenyl esters were precipitated with ether and dried. If not stated otherwise the chemicals were purchased from Aldrich (Steinheim, Germany).

Heterologous expression

The cDNA of the α_1-subunit of the human glycine receptor, inserted in the pCIS expression vector (Gorman et al., 1989), was kindly provided by H. Betz (Max-Planck-Institut for Brain Research, Frankfurt, Germany). Transient transfection of exponentially growing HEK293 cells was performed using the modified calcium phosphate method (Chen and Okayama, 1987) or the Superfect transfection reagent (Qiagen, Hilden, Germany). Cells were co-transfected with cDNA encoding the green fluorescent protein (pGreenLantern, Life Technologies, Gaithersburg, MD) in order to detect transfected cells. Cells were used for electrophysiological experiments 24–60 h posttransfection. The culture of the HEK293 cells was performed

according to published procedures (American Type Tissue Culture Collection, CRL1573).

Electrophysiology

Glycine-induced currents were recorded using the whole-cell configuration (Hamill et al., 1981) and amplified with an Adams and List EPC-7 patch-clamp amplifier. The recording pipette solution contained 120 mM CsCl, 2 mM MgCl$_2$, 10 mM TEACl, 10 mM EGTA, and 10 mM HEPES, and was adjusted to pH 7.3, the bath buffer solution contained 140 mM NaCl, 5 mM KCl, 1 mM MgCl$_2$, 2 mM CaCl$_2$, and 10 mM HEPES (adjusted to pH 7.3). Single-channel currents were recorded using the outside-out membrane patch configuration (Hamill et al., 1981). Membrane potentials were corrected for liquid junction potentials (Barry and Lynch, 1991). Typical pipette resistances were 2.5–3.5 MΩ, the series resistance 4–6 MΩ. Series resistance compensation of 60–80% was used in the whole-cell recording experiments. Typical maximum currents at saturating ligand concentrations were 4–6 nA (whole cells) and 0.2–1 nA (outside-out membrane patches). Whole cells with maximum currents in excess of 6 nA were discarded to avoid holding potential errors related to series resistance (see Results). The high receptor densities necessary for the outside-out membrane patch experiments were achieved by raising the cDNA concentration used together with the Superfect transfection method to 1 μg/ml.

Rapid solution exchange and laser-pulse photolysis

Application of activating ligands and caged compounds to the cells or membrane patches was performed using a rapid solution exchange device (U-tube system, Krishtal and Pidoplichko, 1980). The linear flow rate of the solution emerging from the porthole of the U-tube was 5 cm/s (Niu et al., 1996b). The time resolution, given as 10–90% current rise time, was 20–30 ms with whole cells as determined at supersaturating glycine concentrations and reported previously (Udgaonkar and Hess, 1987).

Laser-pulse photolysis experiments were performed as published earlier (Milburn et al., 1989; Grewer and Hess, 1999). Briefly, the cells were equilibrated with the caged compound for 500 ms before the solution flow was stopped and the laser triggered. The concentration of caged compound ranged between 100 and 500 μM (MNP-derivatives) and 500 μM to 3 mM (αCNB-glycine). The laser light from an excimer laser (λ = 308 nm, pulse duration = 15 ns, Lambda Physik, Goettingen, Germany) or an excimer laser pumped homemade dye laser using p-terphenyl (Lambda Physik, Goettingen, Germany) as laser dye (λ_{max} = 343 nm) was coupled into a 300 μm diameter optical fiber (Laser Components, Santa Rosa, CA), which delivered the laser light to the cell. Laser energies were 50–350 mJ/cm^2. In a typical experiment whole cells or outside-out membrane patches were first rapidly perfused with 1 mM and/or 100 μM glycine solutions using the U-tube device and the maximum current before receptor desensitization was recorded. After 2 min the laser-pulse experiments were performed. After two to three laser-pulse experiments within 1–2 min, typically performed with different concentrations of liberated glycine, the rapid solution exchange experiment was repeated with the same concentration of glycine to control for possible changes in receptor activity or laser-induced damage of the receptors or cells. Experiments obtained from cells with significant change ($>20\%$) of the maximum current after laser-pulse photolysis were discarded. By using this method it is possible to obtain up to 30 laser-pulse photolysis experiments from one cell or membrane patch. To minimize pre-photolytic neurotransmitter release caused by thermal hydrolysis, MNP-β-alanine and αCNB-glycine were freshly dissolved in bath buffer solution (pH 7.3) and the solutions were used for experiments within the next 5–10 min. MNP-glycine was freshly dissolved in unbuffered bath solution (pH adjusted to 4.0) before each experiment. Under these conditions thermal hydrolysis, which takes place with a rate constant of 0.2 min^{-1} at pH 7.4, is relatively slow and the solutions can be stored for several minutes (Ramesh et al., 1993). To prevent thermal hydrolysis at

physiological pH this solution was mixed with a HEPES buffered bath solution 5–10 s before the laser-pulse experiment, using a t-tube mixer (Ramesh et al., 1993) so that the final pH was 7.3.

The amount of neurotransmitter released was controlled using UV-transmissible neutral density filters (Andover Corporation, Salem, NH) and calibrated with the rapid solution exchange method with known concentrations of glycine (Fig. 1 C). Excited-state formation was approximated as a linear function of laser energy within the energy range used. Under the conditions used in these experiments deviation from linearity was always <15% at the highest laser energies, as estimated according to Lachish et al. (1976). The maximum concentrations of released neurotransmitter are limited by 1) background of free neurotransmitter in the caged compounds (≈0.5%), 2) thermal hydrolysis of the MNP-caged derivatives, and 3) laser damage to the cells at laser energies in excess of 450 mJ/cm^2. They were 150 μM for β-alanine and 800 μM for glycine, respectively. The flash/flow system was controlled with the pClamp 6.0 software (Axon Instruments, Foster City, CA). For single-channel recording experiments data were sampled at 30 kHz and filtered at 2–3 kHz (Bessel filter). Laser-pulse photolysis data were sampled with a rate of 10–100 kHz and filtered at 10–20 kHz (Butterworth filter). With a filter setting of 10 kHz (Bessel filter) capacitive injection of a square current pulse into the I-V converter under typical whole-cell recording conditions leads to a 10–90% current rise time of 35 μs.

Data analysis and modeling

Data analysis and nonlinear least-squares fitting was performed with the Origin software (MicroCal, Northampton, MA). For the numerical integration/fitting procedure the Scientist software (Micro Math, Salt Lake City, UT) was used. Single-channel current recordings were analyzed with PClamp 6.0 (Axon Instruments, Foster City, CA).

RESULTS

Measurement of glycine receptor activation with a 100 μs time resolution

In the experiments shown in Fig. 1 A an α_1-receptor expressing cell attached to the recording electrode in the whole-cell current recording configuration (Hamill et al., 1981) was equilibrated with 2 mM caged glycine for 500 ms before photolysis was initiated with a laser pulse at time 0. Glycine release induces a time-dependent current that can be measured with a submillisecond time resolution. Three distinct phases of the current were observed: 1) An initial lag phase occurring on a 0.2–2 ms time scale, 2) a rising phase occurring on a time scale of 0.5–50 ms, and 3) a falling phase of the current on a second time scale. The current is a measure of the channel-open probability, as indicated on the right axis of Fig. 1 A (Hess, 1993), which can be expressed according to the following equation:

$$I(t) = R_0 V_m \sum_i \gamma_i P_{0,i}(t) \tag{1}$$

Here, R_0 represents the number of receptors on the cell surface, V_m the driving force for Cl$^-$ ions, and γ_i and $P_{0,i}$ the conductance and channel-open probability of the ith conductance level, respectively.

Rapid application of glycine or β-alanine to the cells with a fast solution exchange device leads to the activation of similar currents and was used to calibrate the amount of activating ligand released from the caged precursor (Fig. 1 C). Several control experiments demonstrate the validity of the laser-pulse photolysis approach: 1) The glycine-evoked current is inhibited by strychnine. In agreement with results obtained by Bormann et al. (1993) co-application of strychnine (1–10 μM) and glycine (50 μM) induces a current that rapidly decays to the baseline within 200 ms. The maximum current amplitude is inhibited with an inhibition constant of (1.1 ± 0.1) μM (Bormann et al., 1993), suggesting that the glycine-induced current is mediated by the strychnine-sensitive glycine receptor (Langosch et al., 1990). 2) The MNP-derivatives do not activate or inhibit the α_1-glycine receptor at concentrations of up to 500 μM, as demonstrated in Fig. 1 B. Similar results were obtained for αCNB-caged glycine at concentrations of up to 2 mM (this work, data not shown; Grewer, Jäger, Carpenter, and Hess, unpublished results). Thermal hydrolysis of αCNB-caged glycine, which occurs with a time constant of <0.1 h^{-1} can be neglected on the time scale of the laser-pulse photolysis experiment. 3) Photolysis of αCNB-glycine evokes currents that are indistinguishable from those generated by photolysis of MNP-glycine, despite the >2-fold slower photolysis reaction (Grewer, Jäger, Carpenter, and Hess, unpublished results).

Determination of the rate constants associated with the lag and the rising phase

The rising phase of the current can be described with a single exponential function over 85–95% of the total current, indicative of a pseudo-first-order reaction. This is demonstrated in a pseudo-first-order plot (Fig. 1 D, Eq. 2A) which is shown for currents recorded in the outside-out membrane patch configuration. In the whole-cell current recording configuration a minor slow phase of the current rise was observed at intermediate and high concentrations of glycine (data not shown). This phase contributes ~10% to the total current. It is not related to kinetic distortion by series resistance errors (Marty and Neher, 1995) because it is independent of absolute magnitude of the whole-cell current and not affected by series resistance compensation. The nature of this minor component is unknown and only the fast component will be discussed here. The current rise can be described by Eq. 2 under the assumption that the process related to the initial lag phase is in rapid pre-equilibrium.

$$I(t) = I_\infty[1 - \exp(-k_{obs}t)] \tag{2}$$

$$\ln \frac{I_\infty - I(t)}{I_\infty} = -k_{obs}t \tag{2A}$$

In this equation, I_∞ represents the current at $t = \infty$ (in the absence of desensitization) and k_{obs} is the apparent pseudo-first-order rate constant of the current rise. The rate constant, k_{obs}, is obtained from a nonlinear least-squares fit of Eq. 2 to the data. Both whole cells and outside-out patches
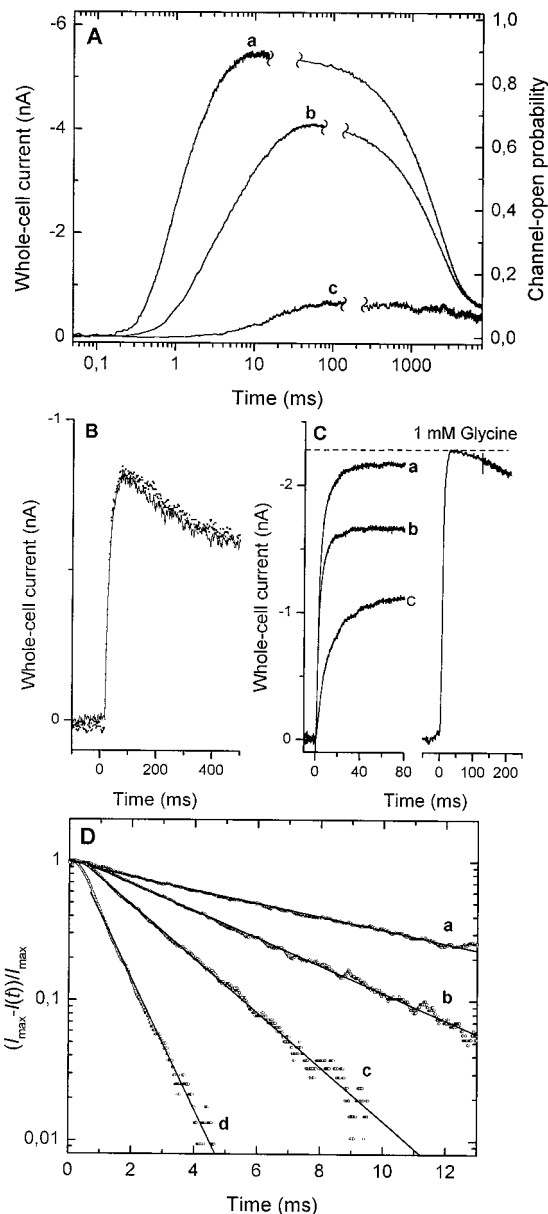
were used for the experiments. The rate constant of the major current rising phase was identical in both cases.

Evaluation of the lag phase is shown in Fig. 2. The glycine concentration was 90 μM. The early phase of the reaction is magnified (note the logarithmic time scale). The measurement of this process is not limited by the time course of photolytic glycine release because of two reasons: 1) The photolysis rate constants of the caged glycine derivatives are $1.7 \cdot 10^5$ and $>3.3 \cdot 10^5$ s^{-1} for αCNB-glycine and MNP-glycine, respectively (Grewer, Jäger, Carpenter, and Hess, unpublished results; Niu et al., 1996a). These rates are at least 2.5 times higher than the highest rate constant of the lag phase at a glycine concentration of 300 μM. 2) The results did not differ for MNP- or αCNB-glycine as caged precursor despite the >2-fold difference in photolysis rate. A sequential kinetic model (Fig. 6) was used to fit the data. The number of occupied binding sites necessary for receptor-channel activation, n, was varied between one and five. For each n the probability of receptor-channels being open was calculated by numerical integration of the system of coupled differential equations (pertaining to the kinetic scheme shown in Fig. 6) and the parameters (k_{+1}, k_{-1}, R) were varied with a numerical

FIGURE 1 (*A*) Typical whole-cell current recordings from α_1-glycine receptor-transfected HEK293 cells after glycine concentration jumps. The receptors were equilibrated with 2 mM αCNB-caged glycine for 500 ms. The laser was triggered at time 0 to generate free glycine concentrations of 300 μM (*trace a*), 110 μM (*trace b*), and 25 μM (*trace c*). The concentration of glycine was calibrated using the cell-flow method (see *C*). The data were low-pass filtered at 20 kHz (4-pole Butterworth filter). The following parameters are associated with the experiments: $I_{max} = (5.5 \pm 0.1)$ nA, $k_{lag} = (4100 \pm 400)$ s^{-1}, $k_{obs} = (1300 \pm 100)$ s^{-1}, $k_d = (0.53 \pm 0.05)$ s^{-1} (*trace a*); $I_{max} = (4.1 \pm 0.1)$ nA, $k_{lag} = (4000 \pm 500)$ s^{-1}, $k_{obs} = (380 \pm 10)$ s^{-1}, $k_d = (0.50 \pm 0.03)$ s^{-1} (*trace b*); and $I_{max} = (0.7 \pm 0.1)$ nA, $k_{lag} = (2300 \pm 300)$ s^{-1}, $k_{obs} = (48 \pm 5)$ s^{-1}, $k_d = (0.11 \pm 0.01)$ s^{-1} (*trace c*). The confidence intervals were obtained from the standard deviation of the parameters given by the nonlinear least-squares fitting routine (Marquardt algorithm, Bevington, 1969). Only the current rise was measured after photochemical glycine release. The falling phase of the current cannot be measured with the implementation of the laser-pulse photolysis technique used here because neurotransmitter diffuses out of the irradiated volume at times in excess of 100–150 ms. Therefore, this phase was measured using the cell-flow method under identical conditions (indicated by the break in the curves). The currents obtained after rapid glycine

application were rescaled with respect to the currents measured after photolytic glycine release to account for small differences in the maximum current amplitudes. The conditions of the experiments were $V_m = -60$ mV, $T = 22°$C, and pH = 7.3. (*B*) Whole-cell currents induced by rapid application of 1 mM glycine to an α_1-glycine receptor-transfected HEK293 cell in the absence (*solid line*) and presence (*symbols*) of 500 μM MNP-caged β-alanine. Similar results were obtained for MNP-caged glycine. The conditions of the experiment were the same as in (*A*). (*C*) Calibration procedure for the determination of neurotransmitter concentration after photolysis. On the left panel whole-cell currents induced by photolytic glycine release from αCNB-glycine are shown. The right panel shows the control experiment performed with the rapid solution exchange method with a glycine concentration of 1 mM. The maximum current amplitude of the control experiment, before receptor desensitization, is indicated by the dashed line and was used to normalize the maximum current obtained from the photolysis experiment. The normalized response was then used to determine the glycine concentration from the known glycine dose response curve (Fig. 7 *B*). By using this procedure the glycine concentrations were estimated as 250 (*trace a*), 100 (*trace b*), and 65 (*trace c*) μM. Concentrations of glycine producing $>90\%$ of saturating current could not be accurately determined with this method. In this case glycine release was estimated by first calibrating with a subsaturating glycine concentration and then increasing the laser energy to release a saturating glycine concentration, assuming that the amount of glycine release is a linear function of laser energy (see Materials and Methods). The error associated with the concentration calibration was assumed to be $\pm 20\%$. Receptor desensitization is slow compared to the current rise and was, therefore, neglected in the calibration process. (*D*) Pseudo-first-order plots of the current rise. $(I_{max} - I(t))/I_{max}$ (Eq. 2A) is plotted as a function of the time. Glycine was released at time 0 from 2 mM αCNB-caged glycine. The data were recorded from membrane patches in the outside-out configuration. The concentrations of glycine were 43 μM (*trace a*), 87 μM (*trace b*), 140 μM (*trace c*), and 275 μM (*trace d*). The rate constants of the current rise, k_{obs}, were obtained from the slope of the linear plots calculated by linear regression analysis. The values are (105 ± 5) s^{-1} (*trace a*), (230 ± 10) s^{-1} (*trace b*), (450 ± 10) s^{-1} (*trace c*), and (1100 ± 20) s^{-1} (*trace d*). The conditions of the experiment were the same as in *A*.
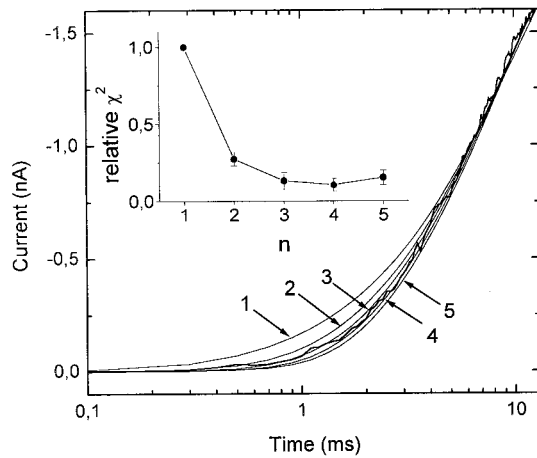
FIGURE 2 Typical whole-cell current recording after photolytic glycine release (*bold trace*) as shown in Fig. 1 *A*. Only the first 12 ms of the reaction are shown to emphasize the lag phase. The concentration of glycine was 90 μM. The data were low-pass filtered at 20 kHz (4-pole Butterworth filter). A numerical integration approach was used to calculate best fits of a sequential *n*-step channel activation model to the experimental data (see Materials and Methods). The number of ligands required for channel activation, *n*, was varied between one and five and the best fits are shown for each value of *n* (*solid lines*). *Inset:* The average sum of least-squares, χ^2, obtained from the numerical least-squares fitting routine, is plotted as a function of *n*. Only the first 15 ms of the current recordings were included in the fit. The χ^2 values are relative values, adjusted to χ^2 at $n = 1$, which was arbitrarily set to 1. The χ^2 values represent the average from three different experiments with different cells. The conditions of the experiments were $V_m = -60$ mV, $T = 22°C$, and pH = 7.3.

TABLE 1 Kinetic parameters of activation and deactivation of the α_1-homomeric glycine receptor by glycine and β-alanine

	Glycine	β-Alanine
n	≥ 3	≥ 3
	$\geq 3*$	$\geq 3*$
K_1 (μM)	95 ± 20	
	$160 \pm 10^{\#}$ **	$360 \pm 15^{\#}$ **
k_{+1} (M^{-1} s^{-1})	$(0.9 \pm 0.1) \cdot 10^{7\|}$	$(0.8 \pm 0.1) \cdot 10^{7\|}$
k_{-1} (s^{-1})	$(1.9 \pm 0.2) \cdot 10^{3\|}$	$(1.8 \pm 0.3) \cdot 10^{3\|}$
k_{op} (s^{-1})	$(2.2 \pm 0.1) \cdot 10^{3}$**	$(2.6 \pm 0.2) \cdot 10^{3}$**
k_{cl} (s^{-1})	38 ± 30**	66 ± 23**
$1/\tau_{op}$ (s^{-1})§	55 ± 16	56 ± 11
	320 ± 70	305 ± 30
ϕ	0.017	0.025
p_0	0.98	0.98
α (s^{-1})¶	0.45 ± 0.1	
k_{+d} (s^{-1})	23.5 ± 6.0	
k_{-d} (s^{-1})	0.04 ± 0.01	
	0.02 ± 0.01** $^{\#\#}$	

Data are results from laser-pulse photolysis experiments, unless stated otherwise. The parameters were determined at -60 mV transmembrane potential. Confidence limits were calculated from the standard deviation of the mean, unless stated otherwise.
*Determined from the lag phase.
$^{\#}$Determined from cell-flow experiments.
§Average results from single-channel recording at 2 and 10 μM agonist.
¶Apparent desensitization rate constant at saturating concentration of agonist, rapid solution exchange experiments.
$^{\|}$Confidence limits obtained from linear regression analysis.
**Confidence limits for parameters obtained from nonlinear least-squares fitting (Marquardt algorithm, Bevington, 1969).
$^{\#\#}$Obtained from the glycine concentration dependence of α.

least-squares fitting routine (see Materials and Methods) until the best fit was obtained. The constants k_{op} and k_{cl} were fixed to the values obtained from the rising phase of the current (Table 1). The theoretical current traces calculated with the optimized parameters are shown in Fig. 2. The inset of Fig. 2 demonstrates that more than two binding sites have to be occupied by activating ligands to induce the conformational change. The sum of squared deviations, χ^2, relative to the value obtained for $n = 1$, is plotted as a function of the number of bound ligands required for channel opening to occur. Clearly, this number is larger than two. Similar results were obtained at two different glycine concentrations, 30 (number of experiments, $N = 3$) and 200 μM ($N = 3$).

Under the assumption that steady-state conditions are applicable for the sum of the closed states $[d(\sum_{i=0}^{n} AL_i)/dt = 0]$, the differential equations pertaining to the reaction scheme shown in Fig. 6 can be integrated analytically. This simplification is valid during the early stages of the reaction when receptor-channel opening can be neglected. The analytical solution for the number of occupied binding sites $n = 3$ is

$$I(t) = I_0 \left[k_{lag}t + \frac{1}{3}\exp(-3k_{lag}t) \right.$$
$$\left. - \frac{3}{2}\exp(-2k_{lag}t) + 3\exp(-k_{lag}t) - \frac{11}{6} \right] \quad (3)$$

where I_0 is a scaling factor and incorporates the apparent rate constant of the receptor-channel opening and k_{lag} represents the observed rate constant associated with the lag phase. Similar procedures have been used to evaluate lag phases of soluble enzymes (Laidler, 1958). By using this approach k_{lag} can be determined with a nonlinear least-squares fit of Eq. 3 to the current recordings.

Concentration dependence of α_1-glycine receptor activation

The rate constant associated with the current rise was measured as a function of glycine concentration over a 40-fold concentration range. The results are shown in Fig. 1 *D* and 3 *A*. Experiments were performed with whole cells and outside-out patches (Fig. 3 *A*) and the results were identical. An increase of k_{obs} from ~ 30 s^{-1} at low glycine concentration to ~ 1500 s^{-1} at 800 μM glycine and -60 mV transmembrane potential is observed. At 800 μM glycine concentration the amplitude of the whole-cell current is saturated (see below). The rate constant, k_{obs}, is not a linear function of glycine concentration. Instead, it saturates at high concentrations of glycine (Fig. 3, *A* and *B*). A sequential kinetic scheme (Fig. 6) was used to describe the data and to derive Eq. 4, which relates k_{obs} to the concentration of the
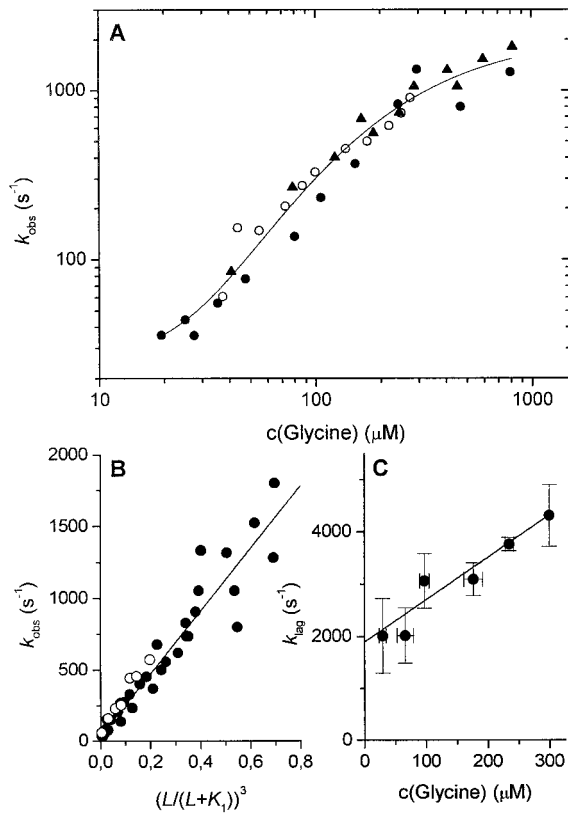
FIGURE 3   Determination of kinetic parameters of the channel-opening process. (*A*) The rate constant of the current rise, k_{obs}, is plotted as a function of the glycine concentration. Experiments with whole cells (*solid and open circles*), and outside-out membrane patches (*triangles*) are shown. The transmembrane potential was -60 mV (*closed symbols*) and 0 mV (*open symbols*). The results at $V_m = -60$ mV were obtained in the absence of a chloride gradient across the cell membrane. At $V_m = 0$ mV the extracellular chloride concentration was 145 mM, the intracellular chloride concentration was 10 mM. Every data point represents the average of at least two experiments with two different cells. The total number of cells evaluated was $N = 55$. The solid line represents a nonlinear least-squares fit of Eq. 4 to the data. The total number of data points included in the fit was 151. The following kinetic parameters were obtained: $k_{cl} = (38 \pm 30)$ s^{-1}, $k_{op} = (2200 \pm 100)$ s^{-1}, $K_1 = (95 \pm 20)$ μM. The confidence limits were obtained from nonlinear regression analysis (Marquardt algorithm). The number of ligands required for receptor-channel activation, n, was set to three. Values of $n = 1$ and 2 did not produce adequate fits to the experimental data. (*B*) The assignment of $n = 3$ is justified by plotting k_{obs} as a function of $(L/(L + K_1))^3$. As expected from Eq. 4 a linear relationship is observed with a slope of (2150 ± 250) s^{-1} and an intercept of (38 ± 30) s^{-1}. The line represents the result from the linear regression analysis. All the data shown in *A* were pooled (*closed symbols*, glycine as activating ligand). The open symbols represent the results from the same experiments performed with β-alanine. Results from a total number of $N = 25$ cells were evaluated. The results with β-alanine as activating ligand were obtained only from whole-cell recordings and at $V_m = -60$ mV. (*C*) Dependence of k_{lag} on glycine concentration. k_{lag} was calculated from a fit of Eq. 5 to the experimental data at each glycine concentration. Each data point represents the average of at least three experiments with three different cells. The line represents the result from linear regression analysis. According to Eq. 5, $k_{+1} = (0.9 \pm 0.1) \cdot 10^7 \, M^{-1} \, s^{-1}$ is obtained from the slope and $k_{-1} = (1900 \pm 200)$ s^{-1} is obtained from the intercept, respectively. The conditions of the experiments were $V_m = -60$ mV, $T = 22°C$, and pH = 7.3.

activating ligand, L.

$$k_{obs} = k_{cl} + k_{op}\left(\frac{L}{L + K_1}\right)^n \tag{4}$$

This equation was derived under the assumptions that the ligand binding steps are in rapid pre-equilibrium and that receptor desensitization is negligible on the time scale of the current rise (see Discussion and Walstrom and Hess, 1994). The rate constants of receptor-channel closing, k_{cl}, and opening, k_{op}, can be determined at low and high concentrations of activating ligand, respectively. The best fit of Eq. 4 to the experimental data was obtained for $n = 3$ (Fig. 3 *B*). However values of $n = 4$ and 5 yielded fits of similar quality (not shown). The relative sum of squared deviations, χ^2, was larger by 1% ($n = 4$) and 2% ($n = 5$) compared to the χ^2 obtained for $n = 3$, respectively. Therefore, it is not possible to differentiate between sequential kinetic models with three, four, and five bound ligands necessary for inducing the conformational change to the open receptor-channel form. The other parameters obtained from the fit are listed in Table 1. The receptor-channel opening rate constant can also be determined by linear regression from the slope of a plot according to Eq. 4, as shown in Fig. 3 *B*. The result does not differ from the one obtained from the nonlinear least-squares fitting routine. Similar results were obtained for β-alanine as activating ligand. Within experimental error the k_{op} and k_{cl} values obtained for β-alanine and glycine are similar. However, the binding affinity was reduced significantly by a factor of $\sim$2.5–3 (Table 1). This result is consistent with the observation that the maximum current at saturating concentration is the same for both activating ligands (Fig. 7 *B*).

The glycine concentration dependence of k_{lag} is shown in Fig. 3 *C*. A linear relationship is observed, consistent with a bimolecular association reaction between glycine and the receptor. The relationship can be described using the following equation:

$$k_{lag} = k_{-1} + k_{+1}L \tag{5}$$

The values estimated from a linear regression analysis for the slope $((0.9 \pm 0.1) \cdot 10^7 \, M^{-1} \, s^{-1})$ and the intercept $(1900 \pm 200 \, s^{-1})$ reflect the rate constants for association of glycine with the receptor, k_{+1}, and glycine dissociation, k_{-1}, respectively.

Voltage-dependence of glycine receptor-channel opening

Whole-cell currents evoked by photolytic release of glycine from the αCNB-precursor were recorded as a function of transmembrane potential. Typical experiments are shown in Fig. 4. The holding potential was varied between -60 and $+60$ mV, while nonsaturating (30 μM) or almost saturating (160 μM) concentrations of glycine were released from αCNB-caged glycine. Two observations are made: 1) Within experimental error, k_{obs} is independent of the trans-
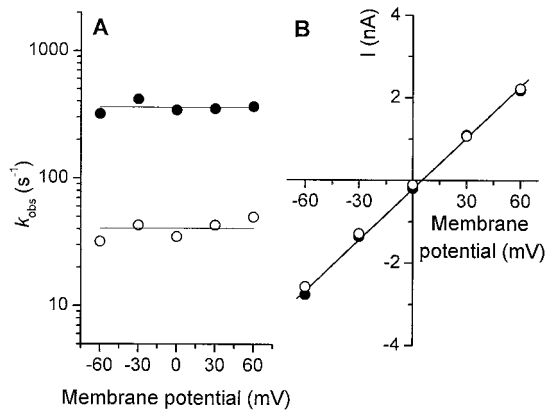
FIGURE 4 (*A*) The rate constant of the whole-cell current rise, k_{obs}, was measured as a function of transmembrane potential at two different glycine concentrations (30 and 160 μM). The results were obtained with two different cells. Similar results were obtained in a total of four experiments with four different cells. The mean rate constants of the current rise, which are represented by the solid lines, are 330 s^{-1} (160 μM glycine) and 43 s^{-1} (30 μM glycine). The conditions of the experiments were $T = 22°C$, and pH = 7.3. (*B*) Voltage-dependence of the whole-cell current amplitude before receptor desensitization. The results were obtained using the cell-flow technique (*open symbols*) and the laser-pulse photolysis technique (*closed symbols*; glycine was liberated from αCNB-glycine) from two different cells. The results obtained with the laser-pulse photolysis technique were calibrated with cell-flow of 1 mM glycine and rescaled with respect to the cell-flow results. The concentration of glycine liberated after the laser pulse was 160 μM.

membrane potential (Fig. 4 *A*). The same results were obtained for a total of $N = 4$ cells. The glycine concentration-dependence of k_{obs} is shown in Fig. 3 *A* at transmembrane potentials of −60 and 0 mV, respectively. Within experimental error the results are identical. 2) The maximum amplitude of the whole-cell current was directly proportional to the transmembrane potential within the voltage range investigated (Fig. 4 *B*). Reversal of the current occurred close to 0 mV, the reversal potential expected for a current carried by the chloride ion in the absence of a chloride gradient across the membrane. These results are consistent with previous reports (Bormann et al., 1993; Sontheimer et al., 1989) and suggest that the channel-open probability and the channel-opening equilibrium constant, as well as the ligand-binding equilibrium constant, are not affected by the transmembrane potential. Therefore, no information about the α_1-glycine receptor gating process can be obtained from relaxation measurements after voltage jumps.

Comparison to single-channel recording experiments

Single-channel currents were recorded from transfected HEK 293 cells using the outside-out membrane patch configuration (Hamill et al., 1981). In the presence of glycine and β-alanine (2 μM–5 mM) single channels were recorded at −60 mV with amplitudes comparable with results reported previously (Bormann et al., 1993; Rajendra et al.,

1995; Takahashi et al., 1992). Typical single-channel recording traces at two glycine concentrations (10 μM and 5 mM) are shown in Fig. 5 *A*. Four conductance levels were observed as reported previously (Rajendra et al., 1995; Bormann et al., 1993). The mean conductance of the main state was (90 $\pm$ 3) pS (Fig. 5 *B*). Only two of these
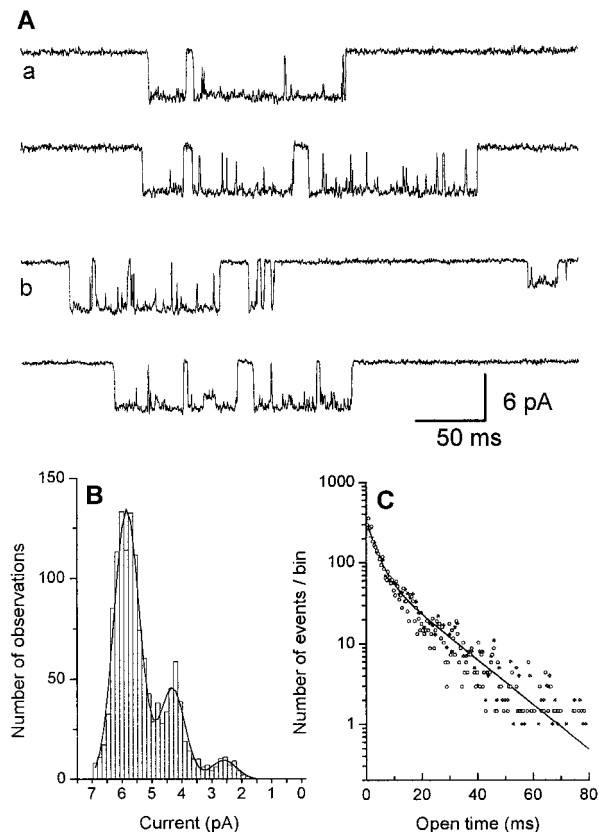

FIGURE 5 (*A*) Typical single-channel recording experiments with glycine as activating ligand. The data were recorded from a membrane patch in the outside-out configuration. The concentrations of glycine used were 5 mM (*trace a*) and 10 μM (*trace b*). The transmembrane potential was −60 mV. The data were low-pass filtered at 3 kHz (Bessel filter). (*B*) Single-channel amplitude histogram at a glycine concentration of 5 mM. A total number of 1320 openings was included in the histogram. The bin width was 0.15 pA. The amplitude distribution was represented by a sum of three Gaussian functions (*solid line*). The single-channel conductances are (97 $\pm$ 1) pS (71%), (72 $\pm$ 1) pS (23%), and (43 $\pm$ 3) pS (5%). (*C*) Open time distribution obtained from single-channel recording experiments at activating ligand concentrations of 10 μM. The data were obtained from a single outside-out membrane patch for glycine and β-alanine, respectively. The open and closed symbols represent results obtained with glycine and β-alanine, respectively. A total number of 3830 (glycine) and 2870 (β-alanine) openings were included in the histograms. The bin width was 1 ms (glycine) and 0.5 ms (β-alanine). The open time distribution obtained for β-alanine was rescaled with respect to the glycine data to show the similar time course. The open time distributions are represented by double exponential decay functions (*solid line*). The following mean open times were calculated from the two exponential components: glycine, $\tau = (3.1 \pm 1.0)$ ms (42%) and $\tau = (17.8 \pm 4.0)$ ms (58%); β-alanine, $\tau = (3.3 \pm 0.3)$ ms (41%) and $\tau = (18.0 \pm 3.0)$ ms (59%). Similar results were obtained at glycine concentrations ranging from 2 to 100 μM from a total of $N = 4$ patches (7200 openings). The conditions of the experiments were $V_m = -60$ mV, $T = 22°C$, and pH = 7.3.

conductance levels contribute to the macroscopic current mediated by glycine activation of the receptor as measured with whole-cell current recording. The highest conductance level carries $\sim$78% of the total current, a conductance level at 66 pS carries 19% of the total current ($N = 3$). The distribution of the single-channel current amplitudes are dependent on the glycine concentration.

Lifetime histograms of the open receptor-channel form are shown in Fig. 5 C for glycine and β-alanine as activating ligand (10 μM). For evaluation of the open-channel kinetics only the main conductance state was used. The lifetime distributions of the open receptor-channel can be represented by a sum of two exponential functions as shown previously for the α_1-homomeric receptor expressed in *Xenopus* oocytes (Takahashi et al., 1992). The mean lifetime of the open channel was determined for the two components, and the values are listed in the legend to Fig. 5 C. The lifetime distribution of the closed channel displays at least three exponential components. A brief, glycine concentration-independent closed time was observed with a time constant of $\sim$0.45 ms (data not shown). This shut state can be assigned to the $(AL)_n$ state (see Fig. 6) with a lifetime of $\tau = 1/(nk_{-1} + k_{op})$ (Colquhoun and Sakmann, 1985). At high concentrations of glycine ($>$100 μM) an additional brief closed time was apparent that was not observed at low agonist concentration. This step is, therefore, concentration-dependent and probably associated with the apparent opening reaction of the receptor (Colquhoun and Hawkes, 1995). The lifetime of this state, which represents the sum of all closed, nondesensitized states, can be expressed as $\tau = 1/[k_{op}L^n/(L + K_1)^n]$. Because of the complicated nature of the multiconductance state single-channel currents, no quantitative evaluation of closed time intervals and burst duration was attempted.

Receptor desensitization

The desensitization process could be represented by a single exponential decay function over the whole glycine concentration range studied (10 μM–5 mM). The relationship between the observed rate constant of receptor desensitiza-
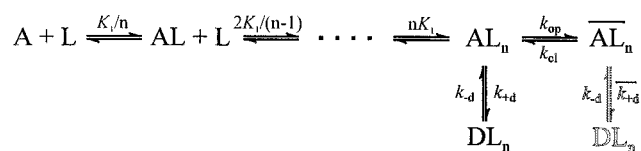
$$A + L \underset{}{\overset{K_1/n}{\rightleftharpoons}} AL + L \overset{2K_1/(n-1)}{\rightleftharpoons} \cdots \overset{nK_1}{\rightleftharpoons} AL_n \underset{k_{cl}}{\overset{k_{op}}{\rightleftharpoons}} \overline{AL}_n$$

with vertical equilibria $k_{-d} \Updownarrow k_{+d}$ to DL_n and $k_{-d} \Updownarrow \overline{k_{+d}}$ to $\overline{DL}_n$

FIGURE 6   Minimal mechanism for activation and desensitization of the α_1-homomeric glycine receptor. A represents the receptor, L the activating ligand; n ligand molecules must bind to induce the conformational change to the open channel form $\overline{AL}_n$. K_1 is the dissociation constant of activating ligand form the receptor with the backward and forward rate constants for ligand binding and dissociation being k_{+1} and k_{-1}, respectively. The channel open equilibrium is characterized by the equilibrium constant Φ and the rate constants for channel opening, k_{op}, and closing, k_{cl}. The slow transition to the desensitized state, DL_n, is characterized by the forward and backward rate constants k_{+d} and k_{-d}.

tion, α, and the glycine concentration is shown in Fig. 7 B. The results were obtained after rapid application of glycine to whole cells using the U-tube device. The rate constant reaches a maximum value of $\sim$(0.45 $\pm$ 0.1) s^{-1} at high glycine concentrations. It can be expressed as a function of
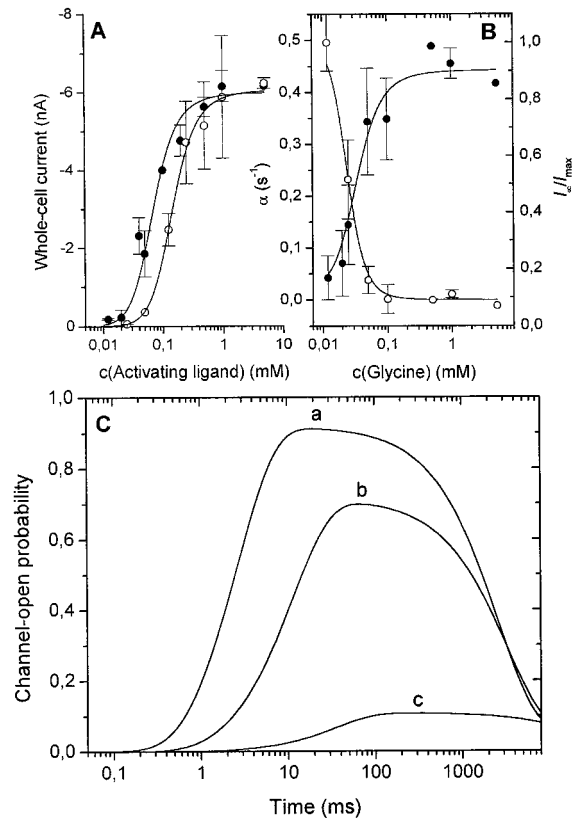

FIGURE 7   (A) Experiments under equilibrium conditions: the maximum whole-cell current amplitude before receptor desensitization is plotted as a function of concentration of activating ligand. Data are shown for glycine (*closed symbols*) and β-alanine (*open symbols*) activation of the receptors. Each data point represents the average of at least three experiments from at least two different cells. The whole-cell current recordings were not corrected for receptor desensitization (Udgaonkar and Hess, 1987) because this process is slow compared to the solution exchange time. The lines represent theoretical curves calculated according to Eq. 7. The parameters used for the calculations are listed in Table 1. The conditions of the experiments were $V_m = -60$ mV, $T = 22°C$, and pH = 7.3. (B) The rate constant of receptor desensitization, α, is shown as a function of glycine concentration (*solid circles*). Rapid solution exchange was used to equilibrate the receptors with glycine (10–20 ms time resolution). The currents were recorded in the whole-cell configuration. The decay of the currents was fitted with a sum of a single exponential decay function and a baseline offset, which accounts for the residual current at $t \to \infty$. The open circles represent the fractional amplitude of the steady-state current after $t > 15$ s with respect to the maximum current amplitude, I_∞/I_{max}. The solid lines were calculated according to Eq. 6 with the parameters obtained from the laser-pulse photolysis experiments (see A) listed in Table 1. The conditions of the experiments were the same as in (A). (C) Simulation of the time-dependent channel-open probability in response to a glycine concentration jump of 300 μM (a), 110 μM (b), and 30 μM (c). The conditions were chosen to match the conditions of the experiments shown in Fig. 1 A. The constants used were $k_{op} = 2200$ s^{-1}, $k_{cl} = 38$ s^{-1}, $k_{+1} = 0.9 \cdot 10^7$ M^{-1} s^{-1}, $k_{-1} = 1900$ s^{-1}, $k_{+d} = 23.5$ s^{-1}, $k_{-d} = 0.02$ s^{-1}, $n = 3$ (Table 1). It was assumed that desensitization takes place only from the closed state, AL_n.

activating ligand concentration according to the following equation:

$$\alpha = \frac{L^n}{L^n + \Phi(L + K_1)^n} \Phi k_{+d} + k_{-d} \qquad (6)$$

Here, k_{+d} and k_{-d} represent the rate constant for formation and back reaction of the desensitized state, respectively (Fig. 6); $\Phi^{-1} = k_{op}/k_{cl}$ is the channel-opening equilibrium constant (Udgaonkar and Hess, 1987). It was assumed that desensitization takes place from the AL_n state. It should be noted that the data are also consistent with a model that involves desensitization from the open-channel state of the receptor. Therefore, this process was included in the model shown in Fig. 6 and printed in light gray. If desensitization takes place only from the open-channel form the intrinsic rate for this process is $\overline{k_{+d}} = \Phi k_{+d}$ (Fig. 6).

Additional information about the receptor desensitization process can be obtained from the steady-state current, I_∞, at times $t \to \infty$, which is a measure of the equilibrium between desensitized and nondesensitized receptor states. This current was measured at times $t > 15$ s after complete receptor desensitization. The ratio of I_∞ and I_{max}, the maximum current before receptor desensitization, is a function of activating ligand concentration and can be expressed as $k_{-d}/\alpha(L)$. The corresponding relationship is shown in Fig. 7 B as the open symbols; k_{-d} was calculated with the relationship $k_{-d} = \alpha I_\infty/I_{max}$ as (0.04 ± 0.01) s^{-1}. Accordingly, k_{+d} was obtained from the known k_{-d} and the value of α at saturating glycine concentrations as (23.5 ± 6) s^{-1} ($\overline{k_{+d}} = 0.4$ if desensitization would occur only from the open-channel form). The parameters were used to calculate the solid lines shown in Fig. 7 A and the agreement is excellent. It should be noted that the number of occupied ligand binding sites required for desensitization to occur is ≥ 3.

A minimal mechanism for glycine receptor activation and desensitization

A five-state sequential model (Fig. 6) was used to simulate glycine receptor-mediated currents. The time-dependent channel-open probability, $P_0(t)$, was calculated by numerical integration of the differential equations pertaining to this mechanism using the parameters listed in Table 1. The simulation is shown in Fig. 7 C for the same glycine concentrations used in the experiment shown in Fig. 1 A. The simulated $P_0(t)$ is similar to the experimental data. In addition, the model was used to represent the concentration dependence of the maximum whole-cell current amplitude, I, which was determined using a rapid solution exchange method. The concentration dependence of I is shown in Fig. 7 A for glycine and β-alanine as activating ligands. Theoretical dose response curves were calculated according to the model using the following equation (Walstrom and Hess, 1994):

$$I = \frac{L^n}{L^n + \Phi(L + K_1)^n} \qquad (7)$$

The thermodynamic and kinetic parameters for the calculation were obtained from the laser-pulse photolysis experiments (Table 1). The results are shown in Fig. 7 A. The experimental and the calculated dose response curves are in good agreement for both glycine and β-alanine as activating ligand.

DISCUSSION

The relaxation of glycine receptor-mediated transmembrane currents reveals three distinct phases after a concentration jump of glycine receptor-activating ligands. The three processes are well-separated on the time scale, ranging from submilliseconds to several seconds (Fig. 1 A). Therefore, at least three receptor reaction steps have to be included into a kinetic scheme to describe the relaxation behavior. The relaxation processes are assigned to these receptor reaction steps by evaluating their characteristic time and concentration-dependence. The most simple kinetic scheme, which is consistent with the results, is analogous to sequential reaction mechanisms first proposed for the nicotinic acetylcholine receptor (Katz and Thesleff, 1957; Hess, 1993). This mechanism is based on three types of structurally different states, which are closed, open, and desensitized (Fig. 6).

The lag phase can be assigned to the ligand-binding step based on two reasons: 1) The rate constant of this process is a linear function of glycine concentration (Fig. 3 C), indicating a bimolecular association process of glycine with the receptor. A bimolecular rate constant for association of glycine with the receptor of $\sim 10^7$ M^{-1} s^{-1} (Table 1) can be estimated, a value one-to-two orders of magnitude smaller than the diffusion limit in aqueous solution. It is at the low end of bimolecular rate constants for small molecule/protein interaction (Hammes, 1982). How does this value compare to ligand/receptor association rates known for other ligand-gated ion channels? Binding of NMDA and glycine to the NMDA receptor occurs with binding rates of $0.8 \cdot 10^7$ M^{-1} s^{-1} and $1 \cdot 10^7$ M^{-1} s^{-1}, respectively (Clements and Westbrook, 1991). Higher binding rates ($>5 \cdot 10^7$ M^{-1} s^{-1}) have been reported for binding of acetylcholine to the muscle type acetylcholine receptor (Liu and Dilger, 1991; Matsubara et al., 1992; Chen et al., 1995). The rate constant for glycine dissociation from the receptor was obtained as 1900 s^{-1}. A value for $K_1 = k_{-1}/k_{+1}$ of 210 μM can be calculated, in reasonable agreement with the value obtained from cell-flow experiments and the effect of glycine concentration on k_{obs} (Table 1). Similar values were obtained for β-alanine as activating ligand (data not shown, Table 1). 2) The time course of the initial lag phase deviates from a first-order reaction. Detailed analysis indicates that three or more glycine molecules are required for receptor-channel opening to occur. In contrast, the receptor-channel opening reaction should obey pseudo-first-order kinetics.

The rate constant, k_{obs}, of the second phase, the current rise, is not a linear function of glycine concentration; instead, it saturates at high glycine concentrations (Fig. 3, A

and *B*). This type of concentration-dependence is typical for a rate-limiting reaction preceded by a rapidly equilibrating ligand-binding step (Hammes, 1982; Eigen, 1968; Matsubara et al., 1992), but should not be observed for a bimolecular ligand association process. For all glycine concentrations used the rate constant of the rising phase is at least five times smaller than the rate constant of the lag phase. It can be, therefore, assumed that pre-equilibrium conditions are valid over the entire concentration range used. The rate constants of receptor-channel opening and closing can be obtained from the limiting values of k_{obs} at high and low glycine concentration as 2200 s^{-1} and 38 s^{-1}, respectively (Fig. 3 *A*, Table 1). The rate constant of receptor-channel opening is five times smaller than the value reported for the muscle-type nicotinic acetylcholine receptor (Matsubara et al., 1992; Liu and Dilger, 1991; Sine and Steinbach, 1986) and about two-to-three times smaller than the opening rate of the GABA receptor in hippocampal neurons (Twyman, 1994; Jayaraman and Hess, 1998). The gating process of the homomeric glycine receptor-channel studied here is, therefore, relatively slow compared to other neurotransmitter receptors of the same superfamily (Betz, 1990).

The maximum rate constant measured for glycine receptor desensitization is similar to previous results obtained with the same receptor (Rajendra et al., 1995) and glycine receptors in native preparations (Akaike and Kaneda, 1989; Walstrom and Hess, 1994). No fast desensitization process on the millisecond time scale was observed. In contrast to experiments performed with *Xenopus* oocytes, only a single exponential current decay was observed (Schmieden et al., 1989). It is, however, possible that the residual current observed at times >10 s after glycine concentration jumps (Fig. 1 *A*) represents another slow desensitization process. Desensitization is, in analogy to open channel formation, a cooperative process and requires three or more ligands bound to the receptor. No evidence for desensitization occurring exclusively from either the open or the closed, but ligand bound state was obtained. Therefore, both processes were included in the kinetic scheme (Fig. 6).

In previous studies glycine receptor activation was investigated under conditions where ligand-binding and channel-gating steps were in quasi-equilibrium, such as the single-channel recording technique (Bormann et al., 1987; Twyman and Macdonald, 1991; Lewis et al., 1998) and methods with rate-limiting glycine application to whole cells or *Xenopus* oocytes (Langosch et al., 1994; Walstrom and Hess, 1994; Lewis et al., 1998). It is shown here that the results obtained with the rapid kinetic technique are in agreement with these data. However, it should be noted that differences exist between the techniques. 1) A short-lived open channel form was observed in single-channel recording data which is not seen in the laser-pulse photolysis experiments. Similar observations were made for the nicotinic acetylcholine receptor (Matsubara et al., 1992; Sine and Steinbach, 1986) and the reason for this is not known. This component might be of importance for the decay of postsynaptic currents. 2) The complexity detected on the single-channel level is absent in the chemical kinetic experiment, where 90% of the opening reaction can be accounted for by a single exponential process. This indicates that minor reaction intermediates, which are seen in single-channel recording experiments, are not detected, leading to a degenerate relaxation spectrum typical for allosteric proteins (Kirschner et al., 1966; Eigen, 1968). Therefore, assignment of rate constants to individual steps of a reaction, as discussed in the previous paragraphs, is straightforward in contrast to analysis of the complex single-channel data recorded from the α_1-glycine receptor.

What are the implications of these studies for the mechanism of ligand-binding and receptor-channel gating? The α_1-glycine receptor forms functional homomultimers (Langosch et al., 1990). The stoichiometry of subunit assembly is not totally clear. It is, however, assumed that a pentameric structure is formed, in analogy to the native glycine receptor (Langosch et al., 1990) and other receptors from the same superfamily (Betz, 1990). The symmetric nature of the subunit assembly, the existence of presumably five identical binding sites for activating ligands, and the ligand-induced transitions between two forms with different quaternary structure are typical for allosteric proteins (Perutz, 1989). Allosteric models were previously proposed for $\alpha\beta$-heterooligomeric glycine receptors (Twyman and Macdonald, 1991; Lewis et al., 1998). The results obtained with the α_1-glycine receptor are consistent with an allosteric activation model. The observation of only three relaxation processes instead of 17 expected for an allosteric model with closed, open, and desensitized states suggests high apparent degeneracy of the relaxation spectrum (Kirschner et al., 1966). It will be interesting to compare these results with other homomeric ligand-gated ion channels such as the 5-HT$_3$ receptor (Neijt et al., 1989), some subtypes of the GABA$_A$ receptor (Sanna et al., 1995), and the α_7-nicotinic acetylcholine receptor (Galzi et al., 1992). None of these receptors has been studied with rapid reaction methods at present. It should be noted that the complex kinetic behavior on the single-channel level with multiple single-channel conductances supports a model with multiple open-channel states (Lewis et al., 1998). However, no evidence in favor of either the allosteric or the sequential activation model was obtained from the rapid chemical kinetic experiments. Therefore, only the more simplistic sequential kinetic model is discussed in detail here, even though it represents an oversimplification.

Native glycine receptors are assembled by α- and β-subunits as heteropentamers (Langosch et al., 1988). It is not totally clear whether α_1-homomeric receptor-channels contribute to currents mediated by glycine receptors at glycinergic synapses. It was, however, proposed that kinetics of homomeric glycine receptors resemble the kinetics of their natively expressed counterparts (Takahashi et al., 1992). Therefore, the α_1-glycine receptor serves as a model system that can be easily studied in heterologous expression systems. Comparison of the kinetic data obtained in this study with kinetic parameters of glycinergic inhibitory postsyn-

aptic currents (IPSCs) shows that 1) the opening rate determined here is consistent with the submillisecond rise time of IPSCs (Stuart and Redman, 1990; Takahashi et al., 1992); 2) IPSC decay time constants measured in adult rat spinal cord preparations are of the same order of magnitude as the lifetime of the long-lived open channel form or the mean burst duration (Takahashi et al., 1992); and 3) glycine receptor desensitization is unlikely to contribute to IPSC decay. However, it should be stressed that kinetic and mechanistic differences might exist between homomeric α_1-glycine receptors and heteromeric $\alpha\beta$-glycine receptors because of different numbers of binding sites for activating ligands (Bormann et al., 1993) and involvement of the β-subunit in the gating process, which is not well studied at present. It will be, therefore, necessary to determine the rate constants pertaining to the receptor activation process with $\alpha\beta$-heterooligomeric glycine receptors in native and heterologous expression systems. This will be done in the future using the laser-pulse photolysis technique. These experiments will give a solid base for the kinetic parameters of the glycine receptor activation process that is necessary to model complicated processes such as glycine-mediated synaptic signal transmission (Kruk et al., 1997).

The laser-pulse photolysis method used in this study provides a useful tool for the investigation of rapid neurotransmitter-mediated receptor reactions. The high time resolution ($\sim 100\ \mu s$) of this method allows the determination of rate constants of individual receptor reaction steps, such as neurotransmitter binding, receptor-channel opening, and desensitization. With the recent development of several suitable caged glycine receptor agonists, the prerequisites for investigation of other glycine receptor subtypes, such as the neonatal α_2-homooligomeric glycine receptor and $\alpha\beta$-heterooligomeric glycine receptors, are fulfilled. The measurement of the rate constants of the channel opening process may help to understand the functional differences between these different receptor subtypes. It will also be possible to compare recombinant receptors expressed in heterologous expression systems to native receptors, not only with respect to ligand-binding affinity, but also with respect to ion-channel gating properties.

REFERENCES

Akaike, N., and M. Kaneda. 1989. Glycine-gated chloride current in acutely isolated rat hypothalamic neurons. *J. Neurophysiol.* 62:1400–1409.

Barry, P. H., and J. W. Lynch. 1991. Liquid junction potentials and small cell effects in patch-clamp analysis. *J. Membr. Biol.* 121:101–117.

Betz, H. 1990. Ligand-gated ion channels in the brain: the amino acid receptor superfamily. *Neuron.* 5:383–392.

Bevington, P. R. 1969. Data reduction and error analysis for the physical sciences. McGraw-Hill Inc., New York.

Billington, A. P., K. M. Walstrom, D. Ramesh, A. P. Guzikowski, B. K. Carpenter, and G. P. Hess. 1992. Synthesis and photochemistry of photolabile N glycine derivatives and effects of one on the glycine receptor. *Biochemistry.* 31:5500–5507.

Bormann, J., O. P. Hamill, and B. Sakmann. 1987. Mechanism of anion permeation through channels gated by glycine and gamma aminobutyric acid in mouse cultured spinal neurons. *J. Physiol.* 385:243–286.

Bormann, J., N. Rundstrom, H. Betz, and D. Langosch. 1993. Residues within transmembrane segment M2 determine chloride conductance of glycine receptor homo and hetero-oligomers. *EMBO J.* 12:3729–3737.

Breitinger, H.-G., and C.-M. Becker. 1998. The inhibitory glycine receptor: prospects for a therapeutic orphan? *Curr. Pharmaceut. Des.* 4:315–334.

Chen, C., and H. Okayama. 1987. High-efficiency transformation of mammalian cells by plasmid DNA. *Mol. Cell Biol.* 7:2745–2752.

Chen, J., Y. Zhang, G. Akk, S. Sine, and A. Auerbach. 1995. Activation kinetics of recombinant mouse nicotinic acetylcholine receptors: mutations of alpha-subunit tyrosine 190 affect both binding and gating. *Biophys. J.* 69:849–859.

Clements, J. D. 1996. Transmitter timecourse in the synaptic cleft: its role in central synaptic function. *Trends Neurosci.* 195:163–171.

Clements, J. D., and G. L. Westbrook. 1991. Activation kinetics reveal the number of glutamate and glycine binding sites on the NMDA receptor. *Neuron.* 7:605–613.

Colquhoun, D., and M. Farrant. 1993. Molecular pharmacology. The binding issue. *Nature.* 366:510–511.

Colquhoun, D., and A. G. Hawkes. 1995. The principles of the stochastic interpretation of ion-channel mechanisms. *In* Single-Channel Recording. B. Sakmann and E. Neher, editors. Plenum Press, New York and London. 31–51.

Colquhoun, D., and B. Sakmann. 1985. Fast events in single-channel currents activated by acetylcholine and its analogues at the frog muscle end-plate. *J. Physiol.* 369:501–557.

Coombs, J. S., J. C. Eccles, and P. Fatt. 1955. The specific ionic conductance and the ionic movements across the motoneural membrane that produce the inhibitory post-synaptic potential. *J. Physiol.* 130:326–373.

Eigen, M. 1968. New looks and outlooks on physical enzymology. *Q. Rev. Biophys.* 1:3–33.

Galzi, J. L., A. Devillers Thiery, N. Hussy, S. Bertrand, J. P. Changeux, and D. Bertrand. 1992. Mutations in the channel domain of a neuronal nicotinic receptor convert ion selectivity from cationic to anionic. *Nature (Lond.).* 359:500–505.

Gorman, C. M., D. Gies, G. McCray, and M. Huang. 1989. The human cytomegalovirus major immediate early promoter can be trans-activated by adenovirus early proteins. *Virology.* 171:377–385.

Grewer, C., and G. P. Hess. 1999. On the mechanism of inhibition of the nicotinic acetylcholine receptor by the anticonvulsant MK-801 investigated by laser-pulse photolysis in the microsecond-to-millisecond time region. *Biochemistry*, in press.

Hamill, O. P., A. Marty, E. Neher, B. Sakmann, and F. J. Sigworth. 1981. Improved patch-clamp techniques for high-resolution current recording from cells and cell-free membrane patches. *Pflugers Arch.* 391:85–100.

Hammes, G. G. 1982. Enzyme Catalysis and Regulation. Academic Press Inc., New York.

Harty, T. P., and P. B. Manis. 1998. Kinetic analysis of glycine receptor currents in ventral cochlear nucleus. *J. Neurophysiol.* 79:1891–1901.

Hess, G. P. 1993. Determination of the chemical mechanism of neurotransmitter receptor-mediated reactions by rapid chemical kinetic techniques. *Biochemistry.* 32:989–1000.

Jayaraman, V., and G. P. Hess. 1998. Transient kinetic investigations of the gamma-aminobutyric acid (GABA) receptor. *Forty-second Annual Meeting of the Biophysical Society, Kansas City, MO.*

Kandel, E. R., J. H. Schwartz, and T. M. Jessell. 1995. Essentials of Neural Science and Behavior. Appleton and Lange, Stanford, CT.

Katz, B., and S. Thesleff. 1957. A study of the "desensitization" produced by acetylcholine at the motor end plate. *J. Physiol.* 138:63–80.

Kirschner, K., M. Eigen, R. Bittman, and B. Voigt. 1966. The binding of nicotinamide-adenine dinucleotide to yeast D-glyceraldehyde-3-phosphate dehydrogenase: temperature-jump relaxation studies on the mechanism of an allosteric enzyme. *Proc. Natl. Acad. Sci. USA.* 56: 1661–1667.

Krishtal, O. A., and V. I. Pidoplichko. 1980. A receptor for protons in the nerve cell membrane. *Neuroscience.* 5:2325–2327.

Kruk, P. J., H. Korn, and D. S. Faber. 1997. The effects of geometrical parameters on synaptic transmission: a Monte Carlo simulation study. *Biophys. J.* 73:2874–2890.

Lachish, U., A. Shafferman, and G. Stein. 1976. Intensity dependence in laser flash photolysis experiments: hydrated electron formation from ferrocyanide, tyrosine, and tryptophan. *J. Chem. Phys.* 64:4205–4211.

Laidler, K. J. 1958. The Chemical Kinetics of Enzyme Action. Oxford at the Clarendon Press, Oxford, U.K.

Langosch, D., C. M. Becker, and H. Betz. 1990. The inhibitory glycine receptor a ligand-gated chloride channel of the central nervous system. *Eur. J. Biochem.* 194:1–8.

Langosch, D., B. Laube, N. Rundstrom, V. Schmieden, J. Bormann, and H. Betz. 1994. Decreased agonist affinity and chloride conductance of mutant glycine receptors associated with human hereditary hyperekplexia. *EMBO J.* 13:4223–4228.

Langosch, D., L. Thomas, and H. Betz. 1988. Conserved quaternary structure of ligand-gated ion channels the postsynaptic glycine receptor is a pentamer. *Proc. Natl. Acad. Sci. USA.* 85:7394–7398.

Legendre, P. 1998. A reluctant gating mode of glycine receptor channels determines the time course of inhibitory miniature synaptic events in zebrafish hindbrain neurons. *J. Neurosci.* 18:2856–2870.

Lewis, T. M., L. G. Sivilotti, D. Colquhoun, R. M. Gardiner, R. Schoepfer, and M. Rees. 1998. Properties of human glycine receptors containing the hyperekplexia mutation α_1(K276E), expressed in *Xenopus* oocytes. *J. Physiol.* 507:25–40.

Liu, Y., and J. P. Dilger. 1991. Opening rate of acetylcholine receptor channels. *Biophys. J.* 60:424–432.

Madsen, B. W., and R. O. Edeson. 1988. Nicotinic receptors and the elusive beta. *Trends Pharmacol. Sci.* 9:315–316.

Marty, A., and E. Neher. 1995. Tight-seal whole-cell recording. *In* Single-Channel Recording. B. Sakmann and E. Neher, editors. Plenum Press, New York and London. 31–51.

Matsubara, N., A. P. Billington, and G. P. Hess. 1992. How fast does an acetylcholine receptor channel open. Laser-pulse photolysis of an inactive precursor of carbamoylcholine in the microsecond time region with Bc-3h1 cells. *Biochemistry.* 31:5507–5514.

Milburn, T., N. Matsubara, A. P. Billington, J. B. Udgaonkar, J. W. Walker, B. K. Carpenter, W. W. Webb, J. Marque, W. Denk, J. A. McCray, and G. P. Hess. 1989. Synthesis photochemistry and biological activity of a caged photolabile acetylcholine receptor ligand. *Biochemistry.* 28:49–56.

Neher, E., and B. Sakmann. 1976. Single-channel currents recorded from membrane of denervated frog muscle fibres. *Nature.* 260:799–802.

Neijt, H. C., J. J. Plomp, and H. P. M. Vijverberg. 1989. Kinetics of the membrane current mediated by serotonin 5 Ht-3 receptors in cultured mouse neuroblastoma cells. *J. Physiol.* 411:257–270.

Niu, L., C. Grewer, and G. P. Hess. 1996b. Chemical kinetic investigations of neurotransmitter receptors on a cell surface in the μs time region. *In* Techniques in Protein Chemistry VII. D. R. Marshak, editor. Academic Press, Inc., New York.

Niu, L., and G. P. Hess. 1993. An acetylcholine receptor regulatory site in BC-3H1 cells characterized by laser-pulse photolysis in the microsecond-to-millisecond time region. *Biochemistry.* 32:3831–3835.

Niu, L., R. Wieboldt, D. Ramesh, B. K. Carpenter, and G. P. Hess. 1996a. Synthesis and characterization of a caged receptor ligand suitable for chemical kinetic investigations of the glycine receptor in the 3-mu time domain. *Biochemistry.* 35:8136–8142.

Perutz, M. F. 1989. Mechanisms of cooperativity and allosteric regulation of proteins. *Q. Rev. Biophys.* 2:139–236.

Rajendra, S., J. W. Lynch, K. D. Pierce, C. R. French, P. H. Barry, and P. R. Schofield. 1995. Mutation of an arginine residue in the human glycine receptor transforms beta-alanine and taurine from agonists into competitive antagonists. *Neuron.* 14:169–175.

Ramesh, D., R. Wieboldt, L. Niu, B. K. Carpenter, and G. P. Hess. 1993. Photolysis of a protecting group for the carboxyl function of neurotransmitters within 3 μs and with product quantum yield of 0.2. *Proc. Natl. Acad. Sci. USA.* 90:11074–11078.

Sanna, E., F. Garau, and R. A. Harris. 1995. Novel properties of homomeric beta-1 gamma-aminobutyric acid type A receptors: actions of the anesthetics propofol and pentobarbital. *Mol. Pharmacol.* 47:213–217.

Schmieden, V., G. Grenningloh, P. R. Schofield, and H. Betz. 1989. Functional expression in *Xenopus* oocytes of the strychnine binding 48-Kd subunit of the glycine receptor. *EMBO J.* 8:695–700.

Sine, S. M., and J. H. Steinbach. 1986. Activation of acetylcholine receptors on clonal mammalian BC3H-1 cells by low concentrations of agonist. *J. Physiol.* 373:129–162.

Sontheimer, H., C.-M. Becker, D. B. Pritchett, P. R. Schofield, G. Grenningloh, H. Kettenmann, H. Betz, and P. H. Seeburg. 1989. Functional chloride channels by mammalian cell expression of rat receptor subunit. *Neuron.* 2:1491–1497.

Stuart, G. J., and S. J. Redman. 1990. Voltage dependence of Ia reciprocal inhibitory currents in cat spinal motoneurons. *J. Physiol.* 420:111–126.

Takahashi, T., A. Momiyama, K. Hirai, F. Hishinuma, and H. Akagi. 1992. Functional correlation of fetal and adult forms of glycine receptors with developmental changes in inhibitory synaptic receptor channels. *Neuron.* 9:1155–1161.

Twyman, R. E. 1994. GABA-A receptor channel opening rates in excised patches of rat cortical neurons. *Jpn. J. Physiol.* 44(Suppl 2):S87–S90.

Twyman, R. E., and R. L. Macdonald. 1991. Kinetic properties of the glycine receptor main-conductance and sub-conductance states of mouse spinal cord neurons in culture. *J. Physiol.* 435:303–332.

Udgaonkar, J. B., and G. P. Hess. 1987. Chemical kinetic measurements of a mammalian acetylcholine receptor by a fast-reaction technique. *Proc. Natl. Acad. Sci. USA.* 84:8758–8762.

Walstrom, K. M., and G. P. Hess. 1994. Mechanism for the channel-opening reaction of strychnine-sensitive glycine receptors on cultured embryonic mouse spinal cord cells. *Biochemistry.* 33:7718–7730.

Werman, R., R. A. Davidoff, and M. H. Aprison. 1968. Inhibitory action of glycine on spinal neurons in the cat. *J. Physiol.* 31:81–95.